species exist in less acid solutions, p*c*H ≥ 1;[4] obviously, more hydrolyzed forms of ruthenium(4.25) can also exist in the same range of acidity since the formal standard potential of the couple ruthenium(4.25)/ruthenium(IV) is independent of the solution acidity. Furthermore, the high charge on these ions most probably is reduced by perchlorate complex or ion-pair formation.

The absorption spectrum of ruthenium(4.25) in 1.0 M $HClO_4$ solution is shown in Figure 4 (this spectrum was recorded immediately after the end of an exhaustive electrolysis of a ruthenium(IV) solution at 1.150 V vs SCE). The spectrum of ruthenium(IV), also shown in Figure 4, is in agreement with earlier literature reports[1,7] ($\epsilon_{486} = 710 \pm 5$). After electrolysis, the absorption maximum in the visible is shifted slightly to longer wavelengths and exhibits a slight increase in absorptivity ($\epsilon_{490} = 730 \pm 5$), in good agreement with the spectrum reported by Avdeev et al.,[10] whereas the shoulder in the ultraviolet has disappeared. Evidently, the spectral changes are rather minimal, and thus absorption spectroscopy certainly is not the most suitable method to measure the presence of small quantities of ruthenium(4.25) in ruthenium(IV) solutions, or vice versa.

Solutions of ruthenium(4.25) in 1.0 M $HClO_4$, stored under "normal" conditions (i.e. in a closed glass container on a lab bench) slowly transformed to ruthenium(IV) (it took several days to obtain 50% conversion). This transformation was ascertained by monitoring the spectral changes and by a series of voltammetric experiments. Thus, the RDE voltammogram of a freshly prepared solution of ruthenium(4.25) in 1 M $HClO_4$ exhibits a wave at 0.800 V vs SCE for the reduction to ruthenium(IV) (of course, the waves for the further reduction of this species are also present in the voltammogram). However, when the solution is allowed to stand, the height of this reduction wave slowly decreases and the height of the oxidation wave at 0.950 V vs SCE slowly increases, thus indicating the formation of ruthenium(IV) (the sum of the heights of both the reduction and oxidation waves remains constant).

Obviously, the only component present in the system that possibly can be oxidized by ruthenium(4.25) is water, but the thermodynamics of this reaction is not favorable. Therefore, it was decided to check qualitatively whether the reaction of ruthenium(4.25) and water is a photochemical process. Indeed, it was found that solutions of ruthenium(4.25) in 1.0 M $HClO_4$ are stable if stored in the dark (the observation period lasted for about 3 weeks, i.e. much longer than the time needed to observe conversion under normal daylight conditions). However, if the solution was irradiated with 254-nm light, transformation of ruthenium(4.25) to ruthenium(IV) was complete in 4–5 h. Thus, while these experiments confirmed qualitatively that the reduction of ruthenium(4.25) to ruthenium(IV) is indeed a photochemical reaction, more work is needed to clarify the photochemistry of this system and the nature of the excited state involved in the reaction.

In solutions of lower acidity, ruthenium(4.25) is quickly transformed to ruthenium(IV), even if the solution is stored in the dark: thus, at p*c*H = 2, the conversion is complete in a couple of hours. Apparently then, under these conditions, ruthenium(4.25) can react directly with water, but the kinetics of this process has not been investigated in detail.

Conclusions

The results of this study confirm the existence of a ruthenium(4.25) species that can be formulated as $Ru_4(OH)_{12}^{5+}$, at least in the more acidic solutions (it is probable that more hydrolyzed species exist in less acidic solutions, p*c*H ≥ 1). The formal standard potential of the ruthenium(4.25)/ruthenium(IV) redox couple was estimated as 1.160 V vs NHE. The redox reaction is independent of the solution acidity and it seems unlikely therefore that the process involves the oxidation of hydroxyl ligands as has been suggested previously.[11] However, any discussion of the bonding in the series of tetrameric ruthenium ions seems premature since the structure of these species in solution remains at present unknown. In 1.0 M $HClO_4$ solution, ruthenium(4.25) can be reduced by water to ruthenium(IV) in a photochemical reaction, but more work is needed to clarify the photochemistry of the process and the nature of the excited state involved in the reaction. In solutions of lower acidity, ruthenium(4.25) is not stable and reacts directly with water (thus, at p*c*H ≥ 2, conversion to ruthenium(IV) is complete in a couple of hours).

Acknowledgment. We are indebted to the Institute for Nuclear Research (IIKW, Brussels, Belgium) for financial support of this work and for granting a research fellowship to one of them (H.V.N.).

Contribution from the Department of Chemistry
and Biochemistry, University of Colorado,
Boulder, Colorado 80309

Catalytic Effect of Sulfur Dioxide on the Electrode Kinetics of the Triiodide/Iodide Couple

Carl A. Koval* and Steven M. Drew

Received April 29, 1988

Halides have been shown to undergo a 1:1 complexation with sulfur dioxide in nonaqueous solvents as seen in reaction 1.[1]

$$X^- + SO_2 = XSO_2^- \qquad (1)$$

XSO_2^- adducts are believed to be charge transfer in nature due to the extremely large molar absorptivities in their electronic spectra.[2] Recently, we have been investigating the electrochemistry of these adducts. More specifically, we were interested in the change in SO_2 binding constant when X^- is oxidized to X_3^-. For this study we chose to use iodide since its electrochemistry in the solvent of interest to us has recently been reported.[3] The report showed that in propylene carbonate I^- undergoes a two-step oxidation to I_3^- and then I_2 via reactions 2 and 3.

$$3I^- = I_3^- + 2e^- \qquad (2)$$

$$2I_3^- = 3I_2 + 2e^- \qquad (3)$$

The I_2/I_3^- couple was shown to have relatively fast rates of electron transfer at a platinum electrode while the I_3^-/I^- couple was quite sluggish, more so for the reduction than for the oxidation. Herein, we report the effects of SO_2 on the thermodynamics of these redox couples and also a surprising improvement in electrode kinetics observed for the reduction of I_3^- at high SO_2 concentrations.

Experimental Section

Materials. Tetrabutylammonium iodide, TBAI, and tetrabutylammonium perchlorate, TBAP (Southwestern Analytical Chemicals), were purified by recrystallization from hot absolute ethanol and dried under vacuum for several days. Propylene carbonate, PC (Aldrich), was purified by vacuum distillation and dried with activated alumina. Anhydrous sulfur dioxide (Air Products) was used without further purification.

Instrumentation. Cyclic voltammetry (CV) and electrolysis/potentiometry measurements were made with a PAR Model 371 potentiostat-galvanostat, Model 379 digital coulometer, and Model 175 universal programmer. Working electrodes were polished platinum or gold, and the auxiliary electrode was a platinum wire. The areas of the working electrodes were estimated by measurement with a ruler under a microscope. All potentials are referenced to ferrocene/ferrocenium by internal standard.[4]

Spectral measurements were made on an HP 8452A diode array spectrophotometer interfaced to a IBM-PC-compatible Zenith computer using HP 89530A MS-DOS/UV-VIS operating software.

Solutions of Sulfur Dioxide. Dilute (≤10^{-2} M) solutions of SO_2 in PC are relatively stable with respect to SO_2 loss. Concentrations of SO_2 in dilute stock solutions (~10^{-2} to ~10^{-3} M) were measured gravimetrically by weighing the solutions before and after addition of gaseous SO_2. Less concentrated solutions were prepared by dilution. The concentration of

---

* To whom correspondence should be addressed.

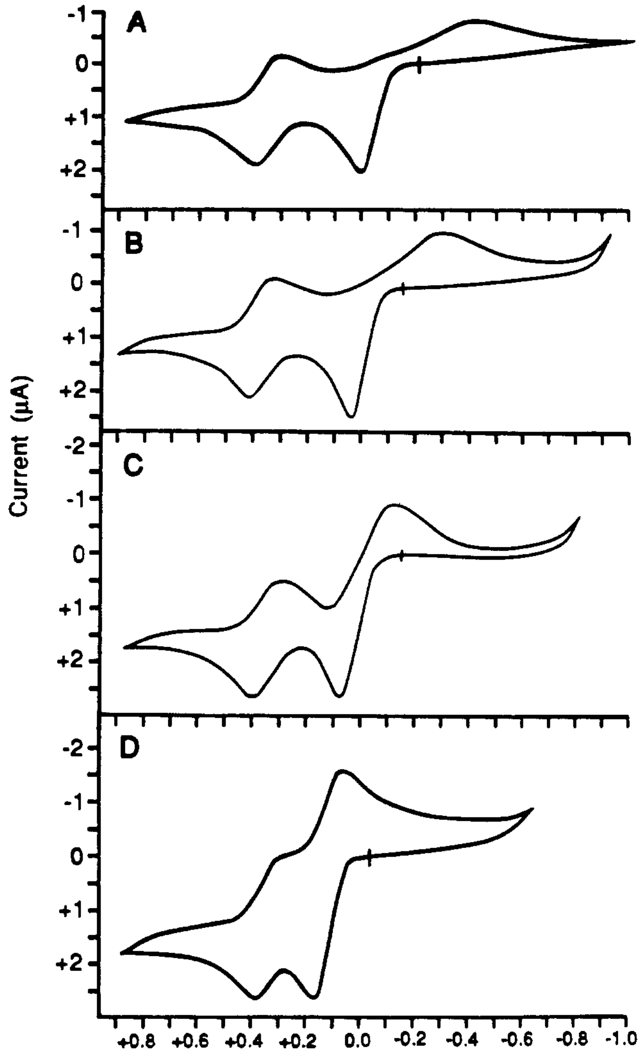

Figure 1. Cyclic voltammetry at a platinum electrode for solutions containing TBAI (4.6 mM) in the absence of SO_2 (voltammogram A) and increasing concentrations of SO_2 (voltammogram B, 0.01 M; voltammogram C, 0.2 M; voltammogram D, 0.9 M (saturated)). All scans initiate in the positive potential direction from the vertical line. The scan rate is 50 mV/s.

saturated solutions was difficult to measure gravimetrically since the solution had to be kept under a constant flow of SO_2. This concentration was therefore estimated by using the Nernst equation (vide infra).

Equilibrium Measurement. The treatment used to obtain a formation constant for ISO_2^- from spectral data was that of Benesi and Hildebrand.[5] For the experimental concentrations employed, $[I^-] \gg [SO_2]$, both a 1:1 complex and the validity of Beer's law for the complex absorbance was assumed. Thus, eq 4 can be applied, where $K_{ISO_2^-}$ is the

$$[SO_2]b/A = 1/\epsilon + 1/\epsilon K_{ISO_2^-}[I^-] \qquad (4)$$

formation constant for ISO_2^-, b is the path length of the cell (cm), A is the absorbance at $\lambda_{max} = 378$ nm for ISO_2^-, ϵ is the molar absorptivity of ISO_2^-, and $[SO_2]$ and $[I^-]$ are initial molar concentrations measured gravimetrically. Absorbances were determined for solutions of constant SO_2 concentration ($\sim 10^{-4}$ M) and varying TBAI concentration ($\sim 10^{-3}$ to $\sim 10^{-2}$ M). A plot of $[SO_2]b/A$ vs $1/[I^-]$ yields a slope of $1/\epsilon K_{ISO_2^-}$ and a y intercept of $1/\epsilon$.

Formal Potential Measurements. Constant-potential electrolysis at a platinum gauze electrode was used to prepare solutions with various $[I_3^-]/[I^-]$ ratios. The potentials of these solutions were recorded, and the formal potentials vs ferrocene were evaluated from the Nernst equation. For the formal potentials measured in solutions saturated with SO_2, SO_2 was continuously bubbled through the solution.

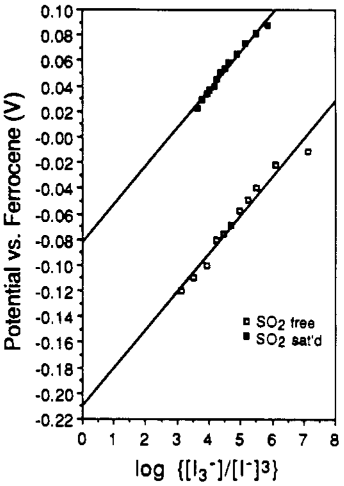

Figure 2. Nernst plots for the I_3^-/I^- couple in the absence of SO_2 (slope = 0.0297) and in a solution saturated with SO_2 (slope = 0.0298).

Results and Discussion

Thermodynamic Effects. The CV's of TBAI at a platinum electrode in PC and in PC containing increasing amounts of SO_2 are given in Figure 1A–D. In solutions free of SO_2 (Figure 1A) the I_3^-/I^- and I_2/I_3^- couples occur as an irreversible wave and quasi-reversible wave with anodic and cathodic peak separations of 0.41 and 0.09 V, respectively. CV's obtained at intermediate to saturated concentrations of SO_2 show an anodic shift in peak potentials for the I_3^-/I^- couple. In contrast, the potential of I_2/I_3^- remains constant within experimental error. Since no anodic shift in the I_2/I_3^- potential is observed, I_3^- must not complex SO_2. Thus, oxidation of ISO_2^- would be expected to follow reaction 5.

$$3ISO_2^- = I_3^- + 3SO_2 + 2e^- \qquad (5)$$

Therefore, the shift in the formal potential for reaction 5 upon the addition of SO_2 is only affected by $K_{ISO_2^-}$ and the concentration of SO_2 in solution.[6] This is shown in eq 6,[7] where $E_{I_3^-/I^-}$ is the

$$E_{I_3^-/I^-,SO_2} = E_{I_3^-/I^-} + 3RT/nF \ln (1 + K_{ISO_2^-}[SO_2]) \qquad (6)$$

formal potential of the I_3^-/I^- couple before the addition of SO_2, $E_{I_3^-/I^-,SO_2}$ is the formal potential of the couple when the solution contains SO_2, and n is the number of electrons in reaction 5. If $K_{ISO_2^-}$, $E_{I_3^-/I^-}$, and $E_{I_3^-/I^-,SO_2}$ are measured independently, the concentration of SO_2 can be calculated from eq 6. This proved to be a useful equation for estimating the concentration of SO_2 at saturation.

$K_{ISO_2^-}$ was measured independently via spectrophotometry by the method described in the experimental section. The results of a Benesi–Hildebrand plot show that $K_{ISO_2^-}$ is 29.6 ± 2.6 M^{-1} in PC that is 0.5 M in TBAP at 25 °C. This is similar to the $K_{ISO_2^-}$ of 21.4 ± 0.4 M^{-1} measured in acetonitrile at 25 °C.[8] The appropriate formal potentials were also measured by using the potentiometric method described in the Experimental Section. A plot of the Nernst equation for reactions 2 and 5 is given in Figure 2 where the y intercept is the formal potential. From Figure 2, $E_{I_3^-/I^-}$ is −0.21 ± 0.01 V and $E_{I_3^-/I^-,SO_2}$ is 0.082 ± 0.005 V when the solution is saturated with SO_2. The slopes of the Nernst plots are expected to be $0.05916/n$ at 25 °C. Again from Figure 2, the slopes indicate that the half-reactions involve 2 electrons.

From the appropriate constants with eq 6, a SO_2 concentration of about 0.89 M at saturation is calculated. The SO_2 concentration

---

(1) Waddington, J. C. *Non-Aqueous Solvent Systems*; Academic: New York, 1965; pp 256–259.

(2) Salama, A.; Salama, S. B.; Sobeir, M.; Wasif, S. *J. Chem. Soc. A* **1971**, 1112.

(3) Hanson, K. J.; Tobias, C. W. *J. Electrochem. Soc.* **1987**, *134*, 2204.

(4) Gagne, R. R.; Koval, C. A.; Lisenski, G. C. *Inorg. Chem.* **1980**, *19*, 2854.

(5) Benesi, H. A.; Hildebrand, J. *J. Am. Chem. Soc.* **1949**, *71*, 2703.

(6) Heyrovski, J.; Kuta, J. *Principles of Polarography*; Academic: New York, 1966; p 157.

(7) Gagne, R. R.; Allison, J. L.; Ingle, M. *Inorg. Chem.* **1979**, *18*, 2767.

(8) Woodhouse, E. J.; Norris, T. H. *Inorg. Chem.* **1971**, *10*, 614.

Table I. Relevant Potentials and SO_2 Concentrations

method	$E_{I_3^-/I^-}$, V	E_{I_2/I_3^-}, V	$[SO_2]$, M
CPE/POT (E^f)	−0.21	0.47[a]	0.0
	−0.082	0.47[a]	0.9[c]
CV ($E_{1/2}$)	−0.022[b]	0.36	0.0
	0.11	0.35	0.9[c]

[a] Determined by using $K_{I_3^-} = 10^{7.7}$ from ref 10. [b] Determined by assuming I^- oxidation is not kinetically limited; thus, $E_{1/2} \cong (E_p + E_{p/2})/2$. [c] Saturated.

of 0.89 M is reasonable in comparison to many other solvents where the solubility of SO_2 is very high, i.e. 0.1–5 M.[9]

Another means of calculating the approximate SO_2 concentration at saturation is to use the difference in potential between the I_2/I_3^- and I_3^-/I^- couple. The difference in these two potentials is indicative of the stability of I_3^- in PC as seen in reaction 7. The

$$I^- + I_2 = I_3^- \qquad (7)$$

potentials are related to the formation constant for I_3^- ($K_{I_3^-}$) by eq 8. A $K_{I_3^-}$ value of $10^{7.7}$ in PC has been reported.[10] From the

$$E_{I_2/I_3^-} = E_{I_3^-/I^-} + 3RT/nF \ln K_{I_3^-} \qquad (8)$$

$E_{I_3^-/I^-}$ value measured here and eq 8, an E_{I_2/I_3^-} value of 0.47 V is calculated. When the solution is saturated with SO_2, reaction 9 is prevalent and the potentials are related to $K_{I_3^-}$ by eq 10. From

$$ISO_2^- + I_2 = I_3^- + SO_2 \qquad (9)$$

$$E_{I_2/I_3^-} = E_{I_3^-/I^-,SO_2} + 3RT/nF \ln \{K_{I_3^-}/(1 + K_{ISO_2^-}[SO_2])\} \qquad (10)$$

eq 10 and the appropriate constants and potentials measured here, the SO_2 concentration at saturation is calculated to be about 0.99 M. This compares favorably with the value previously calculated by using eq 6 and suggests that a SO_2 concentration of about 0.9–1 M is achieved when SO_2 is constantly bubbled through PC.

At first, the formal potentials measured by potentiometry appear to be in conflict with the CV data as seen in Table I. Upon closer examination of the stoichiometry of the half-reactions, it becomes apparent that the potential at half the diffusion limited current, $E_{1/2}$, is not equal to the formal potential, E^f. This is because for stoichiometries of ox:red other than 1:1, the log term of the Nernst equation does not become zero when $E_{1/2}$ is reached. Thus, $E_{1/2}$ only equals E^f for 1:1 stoichiometries. For the I_3^-/I^- couple $E_{1/2}$ will be anodic of E^f due to the 1:3 stoichiometry of the half-reaction. For the I_2/I_3^- couple, $E_{1/2}$ will be cathodic of E^f due to the 3:2 stoichiometry. Determination of the exact separation between $E_{1/2}$ and E^f for these different stoichiometries in CV is not trivial when Nernstian boundary conditions are employed. However, the general trends pointed out above will apply.

Kinetic Effects. As seen in the CV's in Figure 1, the catalytic effect of SO_2 on the reduction of I_3^- is quite substantial. As the SO_2 concentration is increased, the I_3^-/I^- waves shift anodically in an asymmetric fashion. The anodic wave maintains the same general shape; however, the cathodic wave becomes much sharper with the increase in SO_2 concentration. The catalytic effect is maximized when the solution is saturated with SO_2 (~1 M).

Plots of peak current versus scan rate (v = 5–1000 mV/s) are linear with $v^{1/2}$ and not v, suggesting that adsorption is not occurring for the I_3^-/I^- couple with or without SO_2 present. Assuming that the observed peak potentials and currents are kinetic phenomena, the approximate magnitude of the standard rate constant, $k°$, for I_3^- reduction can be determined by varying scan rate. In solutions free of SO_2 (Figure 1A), the I_3^-/I^- couple appears to fit the criteria for a totally irreversible electrochemical reaction. Under these conditions a plot of log of peak current, ln i_p, versus the separation of the thermodynamic potential from the peak potential, $E_p - E°'$, will give a slope proportional to the transfer coefficient, α, and an intercept proportional to $k°$.[11] This should hold true for any stoichiometry since the Nernstian boundary condition is replaced by a kinetic boundary condition and the electrode kinetics will always be first order. The plot shown in Figure 3A gives an approximate α of 0.27 and a $k°$ of 3×10^{-5} cm/s. One specific criterion for an irreversible system is that E_p shifts $-30/\alpha n_a$ mV at 25 °C for every 10-fold increase in scan rate where n_a is the number of electrons for the rate-limiting step.[11] For this system a shift of 110 mV would be expected. For the I_3^-/I^- couple an average shift of 120 mV is observed for scan rates from 5 to 1000 mV/s, indicating that the assumption of irreversibility is valid.

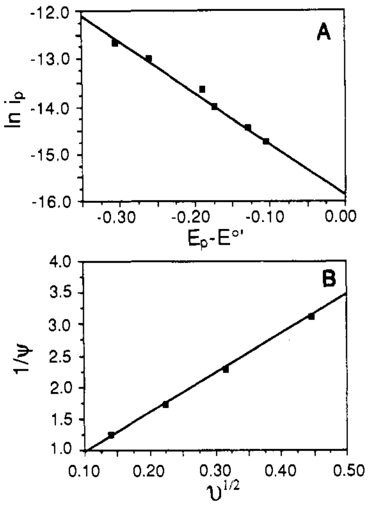

Figure 3. Nicholson plots for the I_3^-/I^- couple in the absence of SO_2 (plot A; slope = −10.5 and y intercept = −15.8) and in a solution saturated with SO_2 (plot B, slope = 6.14). The electrode area is 0.031 cm^2, the concentration of TBAI is 4.1×10^{-6} mol/cm^3, and the diffusion coefficient used is 2×10^{-6} cm^2/s from ref 3.

When the solution is saturated with SO_2 (Figure 1D), the heterogeneous electron-transfer kinetics for the I_3^-/ISO_2^- wave enter the quasi-reversible regime. A method for estimating $k°$ for quasi-reversible waves has been described by Nicholson.[12] Assuming that the kinetic boundary conditions are not greatly affected by stoichiometry, the separation of the anodic and cathodic peak potentials, ΔE_p, will only be affected by v, $k°$, and α. Assuming that I^- and I_3^- have about the same diffusion coefficient, an approximate $k°$ of 4×10^{-3} cm/s is calculated from the plot in Figure 3B by using values of ΔE_p obtained at different scan rates. This is an increase of about 2 orders of magnitude over the $k°$ for the reduction of I_3^- in solutions free of SO_2.

The exact mechanism for this catalytic effect is difficult to ascertain without intensive studies. However, when these experiments are attempted at gold electrodes, a similar catalytic phenomenon is observed. In fact, the kinetics for the I_3^-/I^- couple at gold in the absence of SO_2 are even more sluggish than at platinum, but voltammograms similar to Figure 1D are observed in SO_2-saturated solutions. The electrocatalytic effect is not observed at glassy-carbon electrodes where the kinetics of the I_3^-/I^- couple are even slower. These observations suggest that at high concentrations, SO_2 may chemisorb to the surface of the platinum and gold electrodes and catalyze electron transfer for the I_3^-/I^- couple. However, these variations in the heterogeneous rate constant with electrode material may only be a function of the electrode material itself and not an indication of electrocatalysis.

Acknowledgment. This research is supported by the NSF under Grant No. CBT-8604518. Acknowledgment is also made to the donors of the Petroleum Research Fund, administered by the American Chemical Society.

---

(9) Gerrard, W. *J. Appl. Chem. Biotechnol.* **1972**, *22*, 623.

(10) L'Her, M.; Morin-Bozec, D.; Courtot-Coupez, J. *J. Electroanal. Chem. Interfacial Electrochem.* **1975**, *61*, 99.

(11) Bard, A. J.; Faulkner, L. R. *Electrochemical Methods*; Wiley: New York, 1980; pp 222–224.

(12) Nicholson, R. S. *Anal. Chem.* **1965**, *37*, 1351.